Journal of Magnetic Resonance Open 16–17 (2023) 100120

Contents lists available at ScienceDirect

Journal of Magnetic Resonance Open

journal homepage: www.sciencedirect.com/journal/journal-of-magnetic-resonance-open

The application of solution NMR spectroscopy to study dynamics of two-domain calcium-binding proteins

Roberto Kopke Salinas *

Department of Biochemistry, Institute of Chemistry, University of São Paulo, Av. Prof. Lineu Prestes 748, São Paulo, SP 05508-000, Brazil

ARTICLE INFO

Keywords:
Biomolecular NMR
Protein dynamics
Paramagnetic NMR
Calmodulin
Na+/Ca2+ exchanger
Cadherin

ABSTRACT

Protein dynamics due to flexible linkers connecting otherwise rigid domains may be critical for the functioning of a variety of biological systems, ranging from membrane transporters to calcium-signaling and the formation of intercellular junctions. Considering that NMR spectroscopy is extremely powerful to characterize dynamics at various time scales, this manuscript brings an overview of the main strategies that have been employed to characterize inter-domain dynamics in relevant biological systems. Emphasis was given to the calcium binding proteins: calmodulin, cadherin, and the Na^{+}/Ca^{2+} exchanger calcium-sensor domain. The introduction of paramagnetic centers in diamagnetic proteins is seen as key to obtaining unambiguous information about inter-domain dynamics. This is because the self-alignment of one of the domains in multi-domain proteins avoids the problem of dealing with alignment tensor fluctuations in dynamic systems. The combination of residual dipolar couplings (RDCs) and pseudocontact shifts (PCSs) with computational strategies aiming to provide an ensemble description of protein dynamics is seen as the most powerful strategy to gain detailed atomistic information on inter-domain motions. It is noteworthy that the cadherin ectodomains and the Na^{+}/Ca^{2+} exchanger calcium sensor respond in the same way upon calcium-binding: in the absence of calcium the two domains are flexibly linked to one another and may preferentially sample kinked inter-domain arrangements, while calcium binding stabilizes a rigid and extended inter-domain arrangement. It is thus remarkable that nature chose the same molecular mechanism to promote two very different biological functions that are triggered by calcium signaling: intercellular adhesion by the formation of cadherin dimers and the allosteric regulation of a membrane transporter in the case of the Na^{+}/Ca^{2+} exchanger.

1. Introducion

Calcium ions are key intracellular signaling mediators. They act as second messengers in signal transduction pathways, trigger muscle contraction and induce apoptosis [1–3]. While the extracellular calcium concentration is typically in the mM range, the intracellular calcium concentration is four orders of magnitude lower [3]. The low calcium concentration in the cytosol is key for the signaling roles played by calcium. The sudden opening of calcium passive transport channels after a stimulus causes the intracellular calcium concentration to spike. As a consequence, calcium binds to regulatory proteins that activate a variety of functions. The signal is quenched by the action of calcium-buffering proteins and calcium-extrusion mechanisms, which act to restore the basal intracellular calcium concentration [3,4]. The cytosol contains different soluble proteins that are involved in signaling mediated by calcium, for example calmodulin and protein kinase C (PKC), which have been extensively studied [3,5–7]. Binding of extracellular calcium to adhesion proteins such as cadherins triggers inter-cellular contacts and is required for the formation of intercellular junctions [8,9]. Since the interaction between calcium ions and calcium-dependent signaling proteins is essential for cells functioning, understanding the structural basis of this interaction has always been of great interest. The first calcium-binding motif structurally described was the EF-hand motif identified in parvalbumin [10]. This motif consists of two α-helices separated by a loop that contains one calcium-binding site (Fig. 1). Another widespread calcium-binding motif is the immunoglobulin-like β-sandwich domain, found, for example, in the cadherin extracellular modules. This motif consists of a sandwich of a 4-stranded β-sheet and a 3-stranded β-sheet, and the calcium-binding sites are located at the distal loops of the β-sandwich [11] (Fig. 1). The immunoglobulin-like β-sandwich calcium-binding domain was also called calx-β motif because it was identified in the *Drosophila* Na^{+}/Ca^{2+} exchanger, CALX

* Corresponding author.
E-mail address: rsalinas@usp.br.

https://doi.org/10.1016/j.jmro.2023.100120

Available online 1 May 2023

[12,13]; it differs from the widespread C2 calcium binding domains because the latter consist of a β-sandwich of a pair of four-stranded β-sheets [14].

NMR spectroscopy and X-ray crystallography have given a large amount of information on the structural aspects of the specificity, affinity, and cooperativity of calcium-binding to single domains [3,14]. However, proteins often consist of more than one domain and two or more calcium-binding motifs come together in a single polypeptide chain. It is the change in the relative dynamics or in the average orientation between the domains due to the binding of calcium that triggers the biological function as observed with other modular proteins [17]. Functional protein dynamics have been well characterized in the case of the intracellular calcium-binding protein calmodulin, or the extracellular cadherin ectodomain, and in the case of membrane transporters such as the Na^+/Ca^{2+} exchanger. But obtaining clear and unambiguous evidence of the occurrence of relative domain motions in modular proteins is not trivial, specially when inter-domain linkers are short such that the overall dynamics is coupled with the inter-domain motions [18,19]. Here well understood examples of how NMR spectroscopy was used to investigate relative domain motions, with emphasis on the examples of calmodulin, cadherin, and the Na^+/Ca^{2+} exchanger calcium sensor domain, are reviewed.

2. Calmodulin: a paradigm for two-domain calcium-binding proteins

Calmodulin (CaM) is a small 16.7 kDa protein that is involved in calcium-signaling in the cytosol [6,20]. CaM responds to the sudden increase of the intracellular calcium concentration in excitable cells by binding calcium, and subsequently activating a series of intracellular enzymes [5,7]. CaM was extensively characterized by NMR spectroscopy and X-ray crystallography, in the calcium-free and in the calcium-bound states, and in the ligand-bound state [21–25]. The crystallographic structure of CaM in the calcium bound state shows two globular domains connected by a long α-helix of approximately 8 helical turns, also known as central helix, forming a dumbbell shape [26]. Each globular domain contains two EF-hand motifs, each of them consists of two α-helices separated by a loop that contains a calcium-binding site. Therefore, CaM has four calcium binding sites, two in each one of the two globular domains. Extensions of helix IV in the N-terminal domain and of helix V in the C-terminal domain form the long alpha-helical inter-domain linker [26] (Fig. 2A). Binding of calcium to CaM EF-hand motifs leads to a decrease in the inter-helical angle within each EF-hand, leading to the exposure of hydrophobic residues that were hidden in the unbound state [25,27,28]. This structural change exposes a hydrophobic surface, which prompts CaM to interact with its target sequences. In the calcium-bound state CaM recognizes sequences of approximately 18 amino acids with propensity to form amphipathic alpha-helices [29]. Binding of calcium-loaded CaM to its target peptides leads to the breakage of the central helix, forming two shorter helices separated by a flexible loop, which allows the two globular domains to come close together to embrace the target polypeptide sequence as a clamp, forming a tight complex with a hydrophobic interface [22,30] (Fig. 2B). It is noteworthy that complex formation with the target peptides requires a drastic rigid body motion of CaM two globular domains that assume a compact inter-domain arrangement, which is facilitated by the loss of the helical character in the center of the long inter-domain helix [31] (Fig. 2).

Early on it was noticed that the dumbbell shape observed in the crystallographic structure of the calcium-bound CaM did not agree with the solution structure. Small angle X-ray scattering (SAXS) data showed evidence for a more compact averaged structure in solution [33]. Furthermore, the scattering data obtained for calmodulin in the absence of calcium showed only subtle differences with the calcium-bound state,

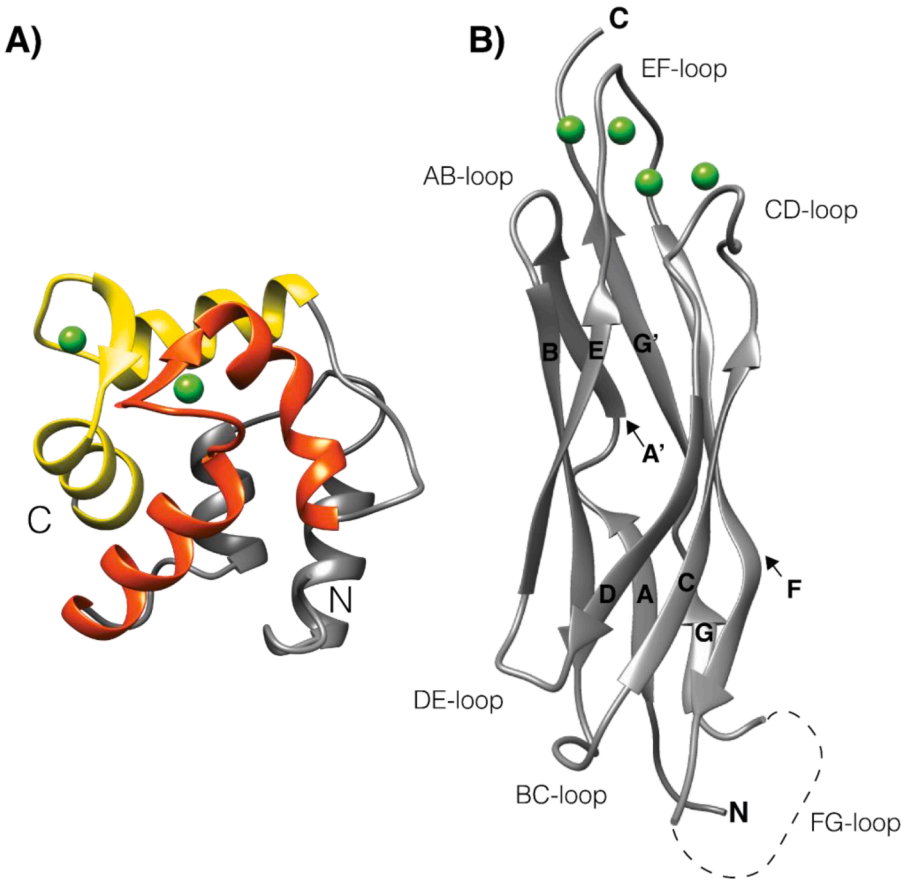

Fig. 1. A) Crystallographic structure of parvalbumin displaying two EF-hand motifs highlighted in red and yellow. PDB: 5CPV [15]. The two EF-hand calcium--binding loops interact with one another forming a short two-stranded β-sheet. **B)** Crystallographic structure of CBD1 (calcium-binding domain 1) from the Na^+/Ca^{2+} exchanger, exemplifying the immunoglobulin-like β-sandwich motif formed by β-sheets G-A-B-E and A'-G'-F-D-C. PDB: 2DPK [16]. Calcium ions are shown as green spheres. N: N-terminal end; C: C-terminal end.

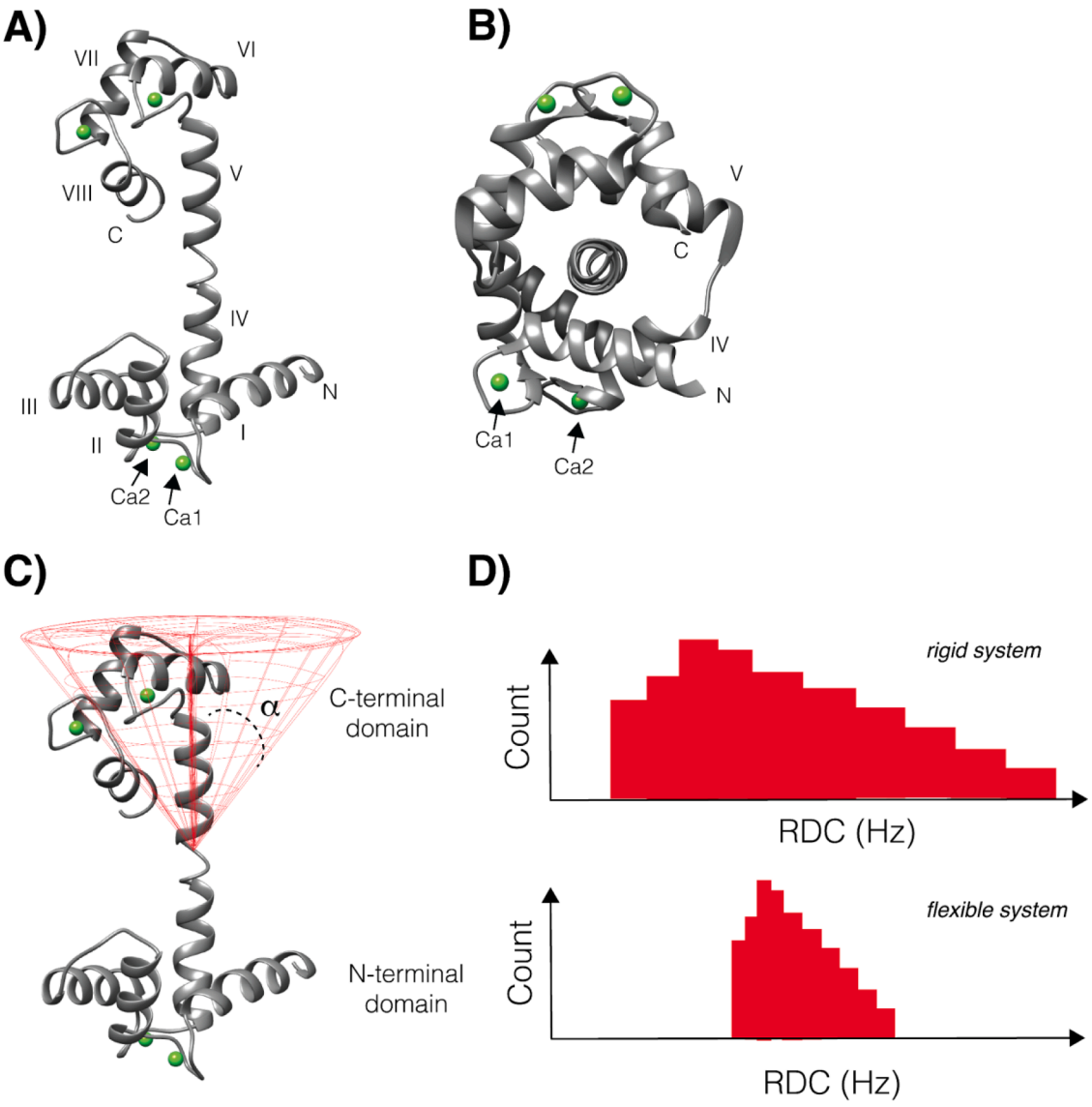

Fig. 2. Inter-domain dynamics in CaM. **A)** Crystal structure of CaM in the calcium-bound state. PDB: 3CLN [26]. Helices IV and V form the long inter-domain helix. **B)** Crystal structure of CaM bound to a peptide analogue of the CaM binding region of the smooth muscle form of myosin light chain kinase. PDB: 1CDL [30]. Calcium binding sites Ca1 and Ca2 at the N-terminal lobe are indicated. The two CaM lobes undergo a large rigid body rotation around the peptide, which is facilitated by the breakage of the long inter-domain helix. **C)** Schematic representation of CaM C-terminal domain motion relative to the N-terminal domain (PDB entry 3CLN). The semi-cone opening angle is an interpretation of the S^2 order parameter of this slow motion modeled by the extended model-free formalism [24]. **D)** Schematic distribution of RDCs measured for the C-terminal domain of a two-domain protein due to the paramagnetic self-alignment of the N-terminal domain in the magnetic field in the absence (top) and presence (bottom) of inter-domain motions. This panel was based on Fig. 4 from reference [32]. Calcium ions are represented by green spheres in **A** and **B**.

namely slightly shorter maximum intramolecular distance (Dmax) and radius of gyration (Rg) values [33]. NMR relaxation data supported the discrepancy between the solution and the crystallographic structures of calmodulin. Specifically, ^{15}N-^{1}H bond vector order parameters (S^2) calculated from longitudinal and transverse ^{15}N relaxation rates and the $\{^{1}H\}-^{15}N$ heteronuclear NOE [34], indicated that the central part of calmodulin inter-domain helix (residues 78 - 81) displayed high flexibility ($S^2 < 0.6$) in the calcium-bound state [21]. The isotropic overall rotational tumbling time (τ_c) of calmodulin, estimated from ^{15}N R_2/R_1 ratios [35], was 7.12 and 6.30 ns for the N-terminal and the C-terminal domains, respectively. Furthermore, isotropic τ_C values for individual NHs were found to be nearly independent of the ^{15}N-^{1}H bond vector orientation in the molecular axis system, suggesting that the overall rotational diffusion tensor was nearly isotropic [21]. Altogether these observations indicated that, in contrast to what would be expected for a rigid protein, CaM two domains reorient at slightly different rates and faster than would be expected for a spherical molecule of similar size [21,35]. In addition, the nearly isotropic rotational diffusion tensor was not consistent with a rigid dumbbell shape. Taken together, these studies supported the view that calmodulin was better described by two domains connected by a flexible hinge, similar to two beads connected by a string. The data also suggested that the average inter-domain arrangement could be more compact as indicated by SAXS [21]. The analyses of calmodulin local and global dynamics were refined using ^{15}N spin relaxation data collected at different static magnetic field strengths, and assuming an axially symmetric overall rotational diffusion tensor [23, 24]. In this case, not only the central helix exhibited characteristics of a flexible linker but the calculation of S^2 order parameters using the Lipari-Szabo model free approach required the introduction of an additional slower rigid body motion using an extended model free approach [36]. It was found that this additional dynamic contribution, attributed to the relative motion of the two domains, had characteristic

τ_c of approximately 3 ns [23,24,36] (Fig. 2C). As pointed out [24], the quantitative analysis of inter-domain motions using the extended-model free approach is, however, not rigorous because the anisotropic overall motion is likely to be modulated by the large scale inter-domain motion [24]. Nevertheless, these early experiments provided solid evidence that CaM was an intrinsically dynamic molecule, displaying large scale inter-domain motions in the calcium-free and in the calcium-bound states. The relative motion between the N-terminal and the C-terminal calmodulin domains is functionally important because the overall closing of the structure around the peptide must be clearly facilitated by the flexibility exhibited by the inter-domain helix and the pre-existing inter-domain motion [31].

Paramagnetic effects induced by the proximity to a paramagnetic center have been used as a source of structural information in the structure calculation of proteins and complexes, and in the characterization of protein dynamics [37–39]. Due to their dependence on the third power (r^{-3}) of the distance between the nucleus and the metal ion, pseudocontact shifts (PCSs) may provide long range distance and angular information (up to 40 - 50 Å) [37,40], which are precious structural data. In addition, the anisotropy of the magnetic susceptibility tensor of the lanthanide ion may be used to weakly align a paramagnetic metalloprotein in the magnetic field, and hence to measure residual dipolar couplings (RDCs) in the absence of an external alignment medium [37,41]. In the case of diamagnetic proteins, lanthanide ions and synthetic lanthanide tags or lanthanide binding peptides may be used to introduce a paramagnetic center [42]. Bertini and co-workers (2003) ingeniously designed a single amino acid substitution to change the selectivity of one of the CaM calcium-binding sites to a lanthanide ion. Remarkably, the N60D mutant was able to selectively bind a lanthanide ion at Ca2, in the second EF-hand motif of CaM N-terminal domain, while three calcium ions occupy the remaining calcium-binding sites [43] (Fig. 2A). The introduction of a single paramagnetic ion allowed the use of paramagnetic effects as tools to investigate CaM inter-domain dynamics [32]. The self-alignment of CaM N-terminal domain at high static magnetic fields due to the magnetic susceptibility anisotropy of the lanthanide ion, made it possible to measure RDCs at the C-terminal domain that were then used to test CaM relative inter-domain motions. This analysis assumed that, if the C-terminal domain experienced motions with respect to the N-terminal domain, RDCs at this domain would be averaged out over all inter-domain orientations, leading to a decrease of the dipolar coupling values in comparison with a situation where the two domains were rigid with respect to one another (Fig. 2D). Indeed, the distribution of RDCs measured for the C-terminal domain of Ca_3Ln-CaM charged with Tb^{3+} and Tm^{3+} was much narrower than that expected for a rigid system, indicating that CaM experienced significant inter-domain motions [32]. This analysis also showed that not all sterically allowed inter-domain orientations were equally probable [32]. Furthemore, since RDCs and PCSs are subjected to motional averaging up to the millisecond time scale, this approach is sensitive to dynamics at much slower time scales than ^{15}N relaxation data. The latter reflect dynamics faster than the overall tumbling at the sub-nanosecond time scale.

The measurement of RDCs as a result of self-alignment at high magnetic fields avoided the complication of dealing with the time modulation of the alignment tensor of a flexible system, permitting a direct investigation of the inter-domain dynamics [32]. However, a structural description of CaM inter-domain motions, i.e. the conformations that are visited, their populations, and the time scales of interconversions, was not obtained. To address this question, the concept of Maximum Allowed Probability (MAP) was introduced to quantify the conformational space sampled by CaM C-terminal domain relative to the N-terminal domain [44]. MAP is equivalent to the largest fraction of time during which a system can visit a given conformation. This approach used a rigid body simulated annealing protocol to minimize a target function corresponding to the difference between experimental and calculated RDCs and PCSs obtained with three different lanthanides. It was found that calcium-bound CaM samples a large number of conformations, none of them with MAP greater than 0.36 and all of them different from the closed conformation found in complexes with peptide ligands [44]. Alternatively, the concept of Maximum Occurrence (MO or MaxOcc) was introduced. As the MAP, the MO concept quantifies the maximum fraction of time a system can spend in a given conformation [45]. The MO idea was implemented to refine a large initial pool of CaM conformers, generating a minimum ensemble of conformations that best fit the experimental data [46], which consisted of a combination of paramagnetic NMR (PCSs and RDCs) and SAXS data. It was found that the extended and the closed CaM inter-domain arrangements may exist for at most 15% and 5% of the time, respectively [46]. The inclusion of double electron-electron resonance (DEER) data in addition to NMR and SAXS information had the effect of favoring a subset of conformations with extended inter-domain arrangements [47]. This approach was further refined by defining the upper and lower occurrence limits, MaxOR and MinOR, respectively, for a given region in the conformational space, and testing this strategy on systems with different degrees of conformational variability [48]. Following a different approach, an ensemble description of inter-domain dynamics was attempted to investigate less flexible systems. The inter-domain dynamics of the complex between CaM and the IQ-recognition motif from the voltage-gated calcium channel $Ca_v1.2$ was characterized by RDCs and PCSs obtained using six different lanthanide ions [49]. An ensemble consisting of the crystal structure and three to four molecular dynamics simulation (MD) snapshots yielded the best agreement with the experimental data, and hence a better description of the dynamics of this system [49]. The dynamics of the complex between CaM and the recognition motif of Munc13–1 was investigated by searching for the minimum ensemble of conformations that best described the experimental data. Samples of Ca_3Ln-CaM in complex with the peptide and six lanthanide ions allowed the measurement of 2691 PCS and RDC restraints for the C-terminal domain, which were used to refine an initial ensemble of 122,700 conformers [50]. The refinement strategy used a genetic algorithm and a fitness function closely related to the Bayesian information criterion, to optimize the conformations, their populations and the ensemble size. This approach yielded ensembles of 7 - 11 conformers and a detailed atomistic description of the CaM-peptide complex inter-domain dynamics [50].

3. Cadherins

Cadherins form a large family of cell surface glycoproteins, many of which participate in calcium-dependent cell adhesion [51,52]. They are formed by an extracellular ectodomain, a transmembrane anchor, and an intracellular C-terminal domain (Fig. 3A). While the ectodomain is involved in intercellular adhesive interactions, the C-terminal domain often interacts with intracellular proteins called catenins [51]. The ectodomain consists of repeating units of approximately 110 amino acids called extracellular cadherins, or EC domains. The EC domains are greek-key motifs whose topology closely resembles that of constant immunoglobulin β-sandwich domains. Each EC domain is formed by seven β-strands arranged in a sandwich of two β-sheets, one composed by β-strands A, G, F and C, and the other by β-strands D, E and B (Fig. 3B and 3C). The N and the C-terminal ends of the EC domains are located at opposite sides of the β-sandwich [11,51,53], facilitating their repeat in tandem. The EC domains are connected to each other by calcium-binding linker regions of approximately 7 - 10 amino acids [51] (Fig. 3B).

Intercellular cadherin adhesion activity depends on the presence of extracellular calcium [8]. Crystallographic structures of tandem EC domains showed three calcium binding sites, Ca1 - Ca3, located between adjacent EC modules. While Ca1 is located at the top of one domain, Ca3 is located at the bottom of the adjacent domain, and Ca2 at the linker between the two EC domains (Fig. 3B). Glu-and Asp-side chain carboxylates in each domain and at the linker make bridging contacts with

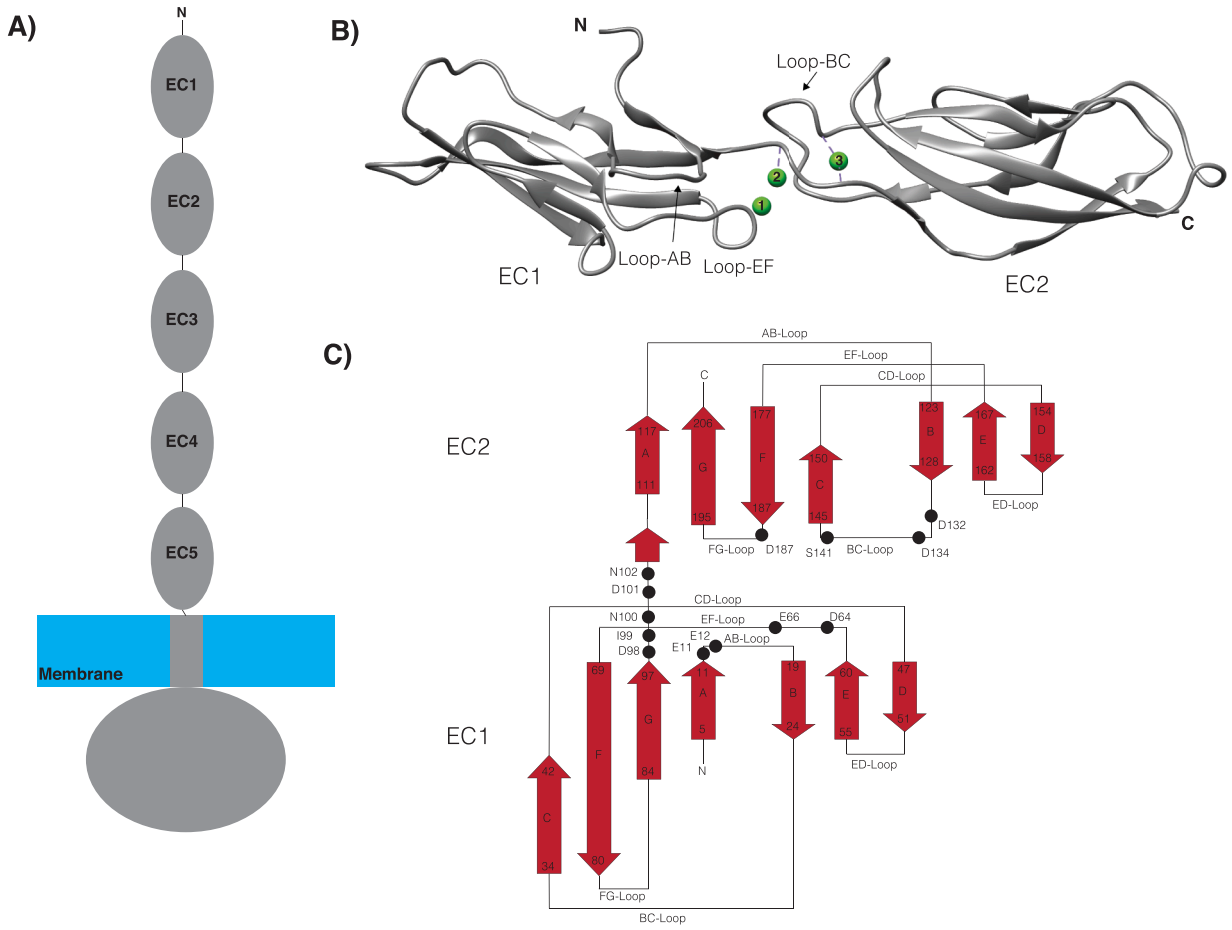

Fig. 3. Structure of cadherin adhesion molecules. **A)** Schematic view of the architecture of classical vertebrate cadherins. The ectodomain is composed of 5 extracellular cadherin (EC) domains (EC1–5) connected to one another by calcium-binding linkers. Cadherins are anchored in the membrane by a single transmembrane helix, and contain an intracellular C-terminal domain. **B)** Crystallographic structure of a two-domain fragment of the mouse cadherin 11 corresponding to the EC1 and the EC2 domains connected by the linker in the calcium-bound state (PDB 2A4E) [53]. This construct is also called EC12 [53]. The calcium binding sites Ca1–3 are indicated by green spheres. Inter-strand loops that form the calcium binding region at the EC12 interface are indicated. **C)** Topology of the EC12 construct. Residues that participate in calcium coordination at sites Ca1–3 are represented by black spheres.

calcium at sites Ca1 and Ca2 or at Ca2 and Ca3, while other residues may coordinate a single ion with their backbone carbonyl group [51–54] (Fig. 3C). Notably, calcium binding was shown to be critical to rigidify an elongated EC inter-domain arrangement [11,54–56], stabilizing the ectodomain in an extended curved shape [55].

The E-cadherin EC12 two-domain construct was well characterized by NMR spectroscopy in the absence and presence of calcium [57,58]. The local and the overall motions of EC12 were investigated by measurements of heteronuclear $\{^1H\}-^{15}N$ NOEs and of ^{15}N longitudinal and transverse relaxation rates. In the absence of calcium, NOE values and relaxation rates were consistent with a Lipari-Szabo S^2 order parameter of 0.5 along the 7-residue inter-domain linker [34], indicating substantial flexibility that could give rise to motions between the two EC domains at the sub-nanosecond time scale [58]. Upon the addition of calcium, resonances in the linker region became broad beyond detection, indicating that calcium binding stabilized the linker and shifted the backbone motions from the nanosecond to the millisecond time scale, where resonances became broader due to intermediate exchange [58]. Analysis of the ^{15}N longitudinal and transverse relaxation rates of EC12 in the calcium free state yielded an isotropic τ_c of approximately 11 ns for the two EC domains, which is slower than that expected for two independent domains but faster than would be expected for a rigid two-domain molecule of the same size [58]. Upon calcium-binding, the overall isotropic τ_c of each domain increased from 11 up to 17 ns, which is consistent with increased restriction of EC12 inter-domain motions due to calcium binding (Fig. 4A). The relative orientation of the two domains was investigated by measurements of ^1H-^{15}N residual dipolar couplings (RDCs) on samples weakly aligned with Pf1 phages [59]. This analysis showed that the mean EC12 conformation in the absence of calcium was kinked. The two domains displayed similar alignment tensors in the presence of calcium, indicating that in the calcium-bound state their relative orientation is similar to that observed in the crystal structure in that condition [58]. Furthermore, the overall alignment of EC1 and EC2 was highly similar in the calcium-bound state, as indicated by the similarity of the principal components of their alignment tensors (A_{zz}), while different A_{zz} values were observed in the calcium-free state (Fig. 4B) [58]. This observation is, on its own, consistent with two domains that are relatively rigid with respect to one another in the presence of calcium, but rather flexible in the calcium-free state. Altogether, the data indicated that while in the absence of calcium EC12 samples different inter-domain arrangements, with a preference for kinked conformations, calcium binding to the EC12 linker stabilizes a relatively rigid and elongated inter-domain arrangement [58].

Cadherin mediated intercellular junctions involve the formation of clusters of cadherin molecules at the cellular surface. These clusters are stabilized by interactions between neighboring cadherins at the surface of the same cell, called *cis* interactions, and by the interactions between cadherin molecules in apposed cells, which are called *trans* interactions [9,51,52]. *Trans* and *cis* cadherin interactions seem to act cooperatively to form intercellular junctions [60,61]. Calcium binding is critical to

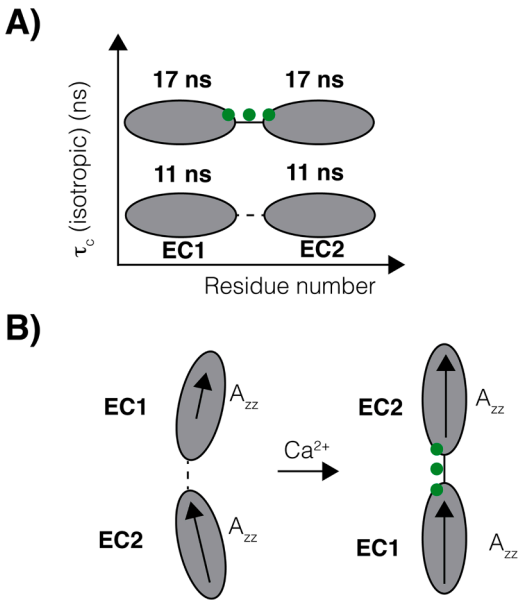

Fig. 4. NMR investigation of inter-domain motions in the EC12 fragment in the absence and presence of calcium [58]. **A)** Analysis of ^{15}N R_1 and R_2 relaxation rates assuming isotropic rotational diffusion yielded the approximate overall tumbling rate of each domain. A faster tumbling rate was observed in the free state in comparison with the calcium-bound state. **B)** Schematic representation of the direction and magnitude of the principal component (A_{zz}) of the alignment tensors of EC12 weakly aligned in the magnetic field. This analysis yielded different alignment tensors for EC1 and EC2, represented by the lengths and the directions of the A_{zz} component, in the free state (left), while the same alignment tensor was observed for the calcium-bound state (right) [58].

stabilize the ectodomains in a rigid and curved shape, allowing the formation of cadherin *trans* dimers between opposed cells [52]. The cadherin *trans* interactions are mediated by the dimerization of the membrane distal EC1 domain [11,51,55,57,61]. A remarkable feature of the EC1 *trans* dimer is the swapping of β-strand A due to binding of Trp2 of Type I cadherins (Trp2 and Trp4 in the case of Type II cadherins) of one monomer into a pocket at the surface of the other monomer [11,53,55] (Fig. 5). NMR spin relaxation experiments provided significant information about the strand-swapping mechanism. Strand-swapped EC1 dimers and monomers were shown to be in slow exchange equilibrium at the NMR chemical shift time scale, which allowed the characterization of the thermodynamics and the kinetics of the strand-swapping process by ZZ-exchange experiments [62,63]. Strand swapping of the EC1 domain from the mouse Type II cadherin 8 was confirmed by ^{15}N-filtered/^{15}N-edited NOESY experiments on mixed ^{14}N- and ^{15}N-labeled samples [62]. β-strand A was shown to be rigid in the sub-nanosecond time scale due to the accommodation of Trp2 and Trp4 in intramolecular and intermolecular hydrophobic pockets in the monomer and in the strand-swapped dimer, respectively [62].

The slow micro to millisecond time scale local dynamics of EC1 and of EC12 constructs was also investigated by NMR. These experiments highlighted possible intermediates along the pathway towards the formation of strand-swapped dimers. Measurements of ^{15}N CPMG relaxation dispersion of the mouse Type II cadherin-8 (8EC1) showed that, in a small population of monomers, β-strand A samples an exposed state, which suggests that strand-exposed conformers could associate to form strand swapped dimers [62]. Extensive measurements of chemical shift perturbations, ^{15}N CPMG relaxation dispersion, chemical exchange saturation transfer (^{15}N CEST) and high-power ^{15}N spin-lock experiments were carried out to characterize the dynamics of wild type and mutant EC1 domains of Type II Cadherin 11 [63]. These experiments revealed that the EC1 monomer undergoes a slow to intermediate time scale chemical exchange process between the main β-strand A-bound state and a sparsely populated partially β-strand A-exposed state, and an intermediate to fast time scale chemical exchange process between the main β-strand A-bound state and a sparsely populated fully β-strand A-exposed state on the pathway to dimerization [63]. Crystallographic structures of two-domain EC12 constructs containing additional non-native residues at the N-terminus, or containing mutations designed to abolish β-strand A swapping, showed that cadherins may form a non-swapped dimer with an elongated shape known as X-dimer. Several lines of evidence support the view that the X-dimers are intermediates along the pathway towards the strand-swapped dimer [64]. Indeed, relaxation dispersion experiments of ^{1}H amide protons provided evidence for the existence of an X-dimer intermediate along the dimerization pathway of the E-cadherin EC12 strand-swapped dimer [65]. The apparent advantage of the X-dimer formation is to decrease the kinetic barrier associated with strand swapping [65].

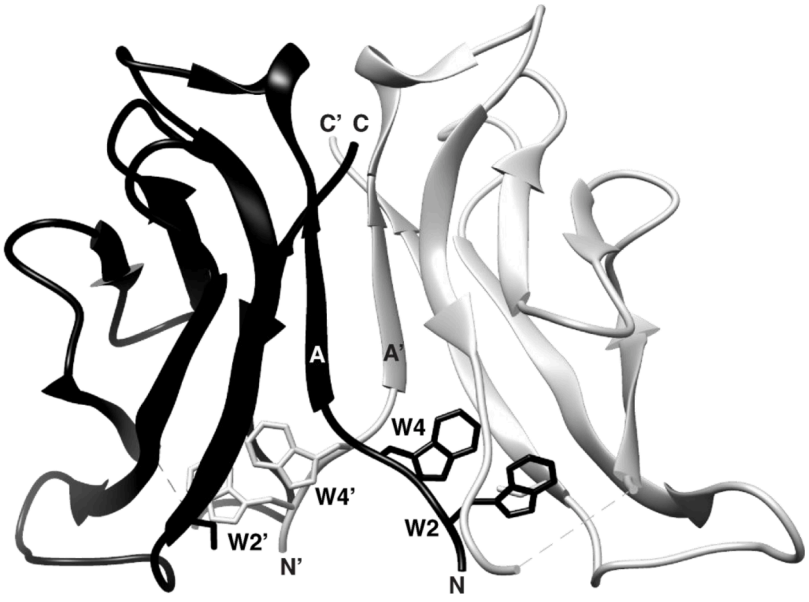

Fig. 5. Crystallographic structure of the strand-swapped dimer of cadherin 8 EC1 domain (PDB 1ZXK) [53]. Swapping of β-strand A is stabilized by the anchoring of W2 and W4 of one monomer in hydrophobic pockets at the surface of the other monomer.

4. The Na^+/Ca^{2+} exchanger calcium sensor domain

The Na^+/Ca^{2+} exchanger (NCX) is an antiporter that couples the transport of sodium downhill its electrochemical gradient to the movement of calcium in the opposite direction against its electrochemical gradient [66,67]. In this way, the NCX is an important calcium extrusion mechanism, especially in excitable cells such as cardiomyocytes [67,68]. In these cells, the NCX contributes to restoring the normal intracellular calcium concentration after a calcium influx caused by the transient opening of calcium channels [68,69]. However, the exchanger may also work in the reverse mode according to the membrane potential and the ionic gradients [67]. The involvement of the NCX in the development of cardiac diseases is well recognized [66,69]. However, new evidence pointing to the NCX involvement in a wider range of pathologies, particularly in neurodegenerative diseases, have been accumulating [66,70]. The NCX transmembrane domain is formed by ten transmembrane α-helices, separated in two homologous and symmetric halves of five transmembrane helices each [71,72]. The two NCX symmetric halves are separated by a large intracellular loop, which connects transmembrane helices 5 and 6. The loop contains an intracellular calcium sensor formed by a tandem repeat of two β-sandwich immunoglobulin-like domains, called calcium-binding domain 1 (CBD1) and calcium-binding domain 2 (CBD2) (Fig. 6A) [73,74]. Three-dimensional structures of the CBDs in isolation and in the two-domain CBD12 construct were obtained by X-ray crystallography or by NMR spectroscopy [16,75–81]. Similarly to the cadherin EC12 construct (Fig. 3B), CBD12 assumes an extended inter-domain arrangement in the calcium-bound state (Fig. 6B). The CBD12 inter-domain interface is formed by the packing of the interstrand EF-loop of the CBD1 domain, against the BC and the FG interstrand loops of CBD2 and the inter-domain linker [78,79] (Fig. 6B). CBD12 binds four calcium ions at the distal loops of the CBD1 β-sandwich and no direct contribution from CBD2 to calcium coordination near the inter-domain linker is seen (Fig. 6C) [78,79].

The local backbone dynamics of the CBD1, CBD2 and CBD12 constructs were characterized by solution NMR spectroscopy [83–88]. Measurements of Lipari-Szabo S^2 order parameters of the backbone ^1H-^{15}N bond vectors showed that binding of calcium restricts slightly the dynamics of the inter-strand loops in the calcium-binding regions of CBD1 and CBD2 from the canine exchanger [83,84]. In the absence of calcium, backbone resonances for residues located in the CBD1 calcium binding region of the *Drosophila* exchanger, CALX, were missing probably due to exchange broadening [87]. However, they appeared upon the addition of calcium, indicating that, also in the case of the *Drosophila*

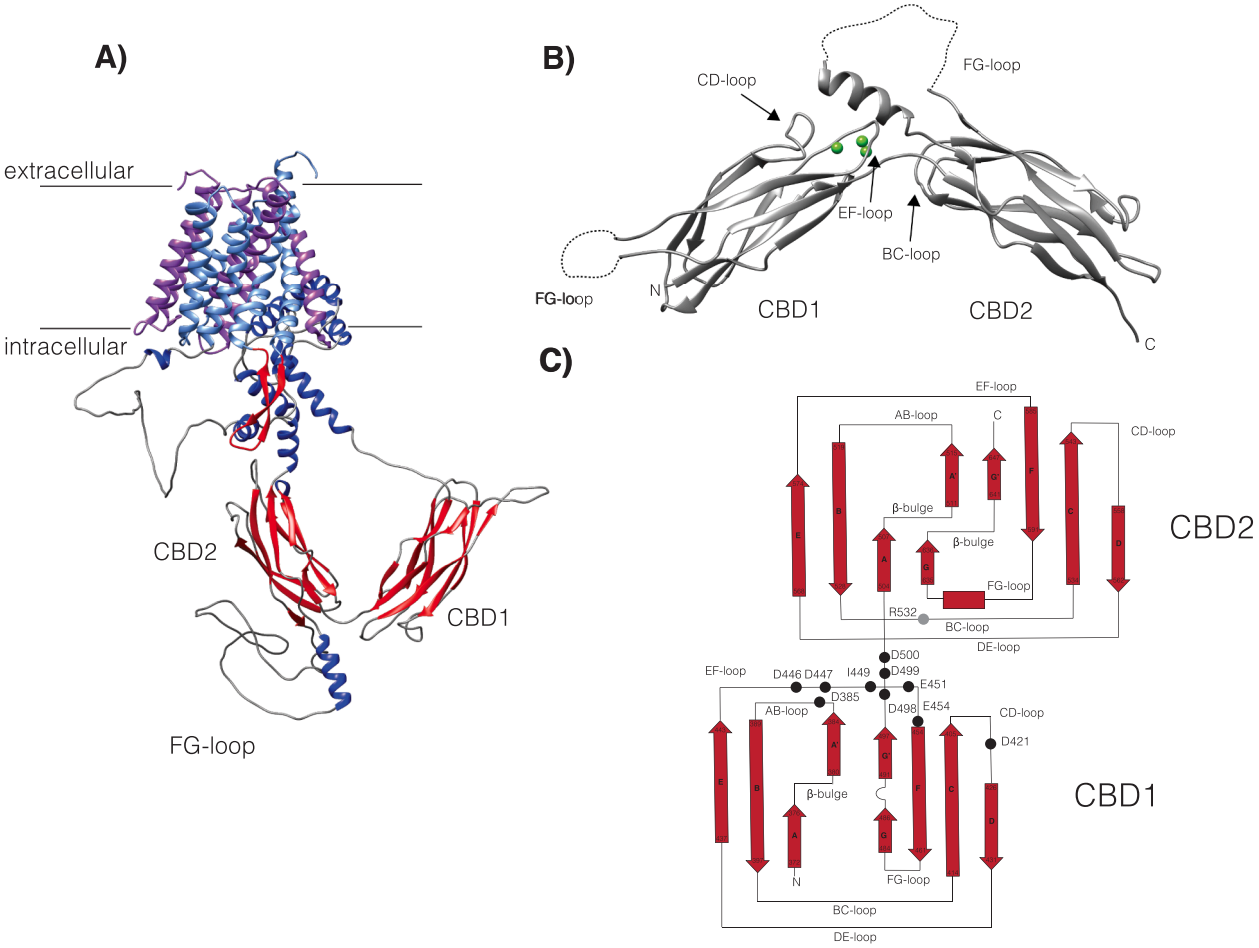

Fig. 6. Architecture of the Na^+/Ca^{2+} exchanger. **A)** Prediction of the three-dimensional structure of the complete canine NCX using ColabFold [82]. While the quality of this prediction is uncertain, it shows how CBD12 could be connected to transmembrane helices 5 and 6 by a folded helical domain and disordered linkers. The transmembrane domain, and the disordered FG-loop from CBD2 are indicated. **B)** Crystallographic structure of the CBD12 construct from the canine NCX (PDB 3US9) [78]. Calcium ions are represented by green spheres. Loops for which no electron density was observed are represented by segmented lines. The inter-strand loops that make part of the two-domain interface are indicated. This construct corresponds to a mutant, E454K, which explains why three instead of four calcium ions were observed. **C)** Topology of the CBD12 construct based on the crystal structure (PDB 3US9). Residues that participate in calcium coordination with the side chain carboxylate groups or with the backbone carbonyl group are indicated by black spheres. R532 in the CBD2 BCE-loop (colored gray) does not participate in calcium coordination, but it makes salt bridges with D500 and D499 in CBD1 and with D565 in CBD2 [78].

exchanger, calcium binding to CBD1 leads to rigidification of the calcium-binding loops [87]. Furthermore, measurements of transverse and longitudinal ^{15}N relaxation rates of CBD12 showed that calcium binding increased the isotropic τ_c of CBD1 and CBD2 from approximately 14 ns and 17 - 19 ns in the calcium-free state up to 20 ns and 33 ns in the calcium-bound state, for the canine and the *Drosophila* CBD12 constructs, respectively [85,86]. Measurements of ^{1}H-^{15}N RDCs on weakly aligned CBD12 samples indicated that the CBDs assume an extended inter-domain arrangement in the presence of calcium, in good agreement with the CBD12 crystallographic structures [85,86]. Altogether, these findings are consistent with the view that calcium binding to CBD12 restricts the inter-domain dynamics in the sub-nanosecond time scale, stabilizing a rigid and extended inter-domain orientation in analogous manner as that observed for the EC12 construct (Fig. 4) [58]. RDCs and SAXS data, and long 3.4 μs MD trajectories were used to investigate the inter-domain dynamics of the *Drosophila* CBD12 construct in the calcium-free state. The MD snapshots that best agreed with the experimental RDCs were kinked, suggesting that the *Drosophila* CBD12 preferentially samples kinked conformations in the calcium-free state [88]. As an attempt to interpret the CBD12 inter-domain dynamics in terms of an ensemble of conformers, a pool of CBD12 MD snapshots chosen according to their agreement with the RDCs, was further refined with SAXS data using the Ensemble Optimization Method (EOM) [89]. This analysis yielded a minimum ensemble of three CBD12 snapshots, which included kinked and extended inter-domain arrangements with a higher weight for the former, that explained the SAXS data obtained for the calcium-free state [88].

Electrophysiology experiments showed that the binding of calcium to CBD12 triggers activation of the NCX [16,68,76,90]. Curiously, calcium binding to CBD12 inhibits the exchanger from *Drosophila*, CALX [91,92]. The *Drosophila* exchanger is unusual, since it is the only exchanger characterized to date that is inhibited by calcium binding to CBD12. CBD1 is considered to be the primary calcium sensor of the NCX because it binds calcium with greater affinity than CBD2 [16,93]. A three-dimensional structure of the full length exchanger is not available, but a prediction using ColabFold [82] and the NMR structure of a fragment corresponding to the linker between the CBD1 domain and TM5 [94], suggest that the CBD12 calcium sensor is connected to TM5 and to TM6 by an alpha-helical linker domain and disordered segments (Fig. 6A) [86,94]. A model to explain the calcium regulation of the exchanger was proposed, according to which calcium binding to CBD1 stabilizes an extended inter-domain arrangement between the two CBDs, causing a tension on the transmembrane helices and eventually activating (NCX) or inhibiting (CALX) the ion transport activity [86,94].

5. Conclusions and outlook

Protein dynamics due to flexible linkers connecting otherwise rigid domains may be critical for function of a variety of biological systems, ranging from membrane transporters, to calcium-signaling and the formation of adherent junctions [31,58,88]. Although the NCX CBD12 calcium-sensor and the cadherin EC12 dimerization module display the same folding, their calcium-binding modes differ: EC12 displays three calcium binding sites at the inter-domain interface [53], while CBD12 binds four calcium ions at the distal loops of the CBD1 β-sandwich and no direct contribution from CBD2 to calcium coordination is seen (Figs. 3 and 6) [78,79]. The inter-domain interfaces of CBD12 and EC12 constructs in the calcium-bound state are also different: the EF interstrand loop of the EC1 domain and the EC2 BC-loop pack against the inter-domain linker (Fig. 3) [52,53], and while these features are preserved the CBD2 FG-loop makes important contacts with CBD1 in the CBD12 interface [78,79]. Despite these differences, EC12 and CBD12 respond in the same way upon calcium-binding: in the absence of calcium the two domains are flexibly linked to one another and may preferentially sample kinked inter-domain arrangements, while calcium binding stabilizes a rigid and extended inter-domain arrangement. It is thus remarkable that nature chose the same molecular mechanism to promote two very different biological functions triggered by calcium signaling: intercellular adhesion by the formation of cadherin dimers and the allosteric regulation of a membrane transporter in the case of the Na^{+}/Ca^{2+} exchanger.

It is likely that paramagnetic NMR will play a major role in the characterization of intramolecular motions. The chemical shift modulation induced by the proximity with a paramagnetic center in flexible systems has been exploited in combination with R_2 dispersion methods to characterize domain motions, yielding populations and rates of interconversion [39,95]. Nevertheless, a complete characterization of inter-domain dynamics requires description of the conformations of all accessible states, their populations and the rates of interconversion, in other words, of the conformational energy landscape of the molecule. As observed in this review, the combination of advanced computational methods to explore the conformational energy landscape and to select the most probable conformers based on experimental data was crucial to obtain one possible ensemble description of CaM dynamics [50]. This task is challenging, especially for systems that are highly flexible and that display almost a continuum of different conformations [96], but it should be also pursued to characterize inter-domain dynamics involving immunoglobulin-like β-sandwich calcium-binding modules.

Declaration of Competing Interest

The authors declare that they have no known competing financial interests or personal relationships that could have appeared to influence the work reported in this paper.

Data availability

No data was used for the research described in the article.

Acknowledgements

The author thanks Dr. S. Tomaselli (SCITEC, CNR, Italy) for critical discussions about this manuscript. This work was supported by the São Paulo Research Foundation (FAPESP grant #2019/19968–1). RKS receives a research fellowship from the Conselho Nacional de Desenvolvimento Científico e Tecnológico (CNPq #308119/2020–7).

References

[1] E. Carafoli, Calcium signaling: a tale for all seasons, Proc. Natl. Acad. Sci. U.S.A. 99 (2002) 1115–1122, https://doi.org/10.1073/pnas.032427999.
[2] D.W. Choi, Calcium-mediated neurotoxicity: relationship to specific channel types and role in ischemic damage, Trends Neurosci. 11 (1988) 465–469, https://doi.org/10.1016/0166-2236(88)90200-7.
[3] E. Carafoli, J. Krebs, Why calcium? How calcium became the best communicator, J. Biol. Chem. 291 (2016) 20849–20857, https://doi.org/10.1074/jbc.R116.735894.
[4] E. Carafoli, The homeostasis of calcium in heart cells, J. Mol. Cell. Cardiol. 17 (1985) 203–212, https://doi.org/10.1016/S0022-2828(85)80003-1.
[5] A. Villalobo, H. Ishida, H.J. Vogel, M.W. Berchtold, Calmodulin as a protein linker and a regulator of adaptor/scaffold proteins, Biochimica et Biophysica Acta (BBA) - Mol. Cell Res. 1865 (2018) 507–521, https://doi.org/10.1016/j.bbamcr.2017.12.004.
[6] J. Haiech, M. Moreau, C. Leclerc, M.-.C. Kilhoffer, Facts and conjectures on calmodulin and its cousin proteins, parvalbumin and troponin C, Biochimica et Biophysica Acta (BBA) - Mol. Cell Res. 1866 (2019) 1046–1053, https://doi.org/10.1016/j.bbamcr.2019.01.014.
[7] A.B. Sorensen, M.T. Søndergaard, M.T. Overgaard, Calmodulin in a heartbeat, FEBS J. 280 (2013) 5511–5532, https://doi.org/10.1111/febs.12337.
[8] M. Takeichi, The cadherins: cell-cell adhesion molecules controlling animal morphogenesis, Development 102 (1988) 639–655, https://doi.org/10.1242/dev.102.4.639.
[9] S.M. Troyanovsky, Adherens junction: the ensemble of specialized cadherin clusters, Trends Cell Biol. (2022), https://doi.org/10.1016/j.tcb.2022.08.007. S0962892422002094.
[10] R.H. Kretsinger, C.E. Nockolds, Carp muscle calcium-binding protein, J. Biol. Chem. 248 (1973) 3313–3326, https://doi.org/10.1016/S0021-9258(19)44043-X.

[11] L. Shapiro, A.M. Fannont, P.D. Kwong, A. Thompson, Structural basis of cell-cell adhesion by cadherins, Nature 374 (1995) 327–337, https://doi.org/10.1038/374327a0.

[12] E.M. Schwarz, S. Benzer, Calx, a Na-Ca exchanger gene of Drosophila melanogaster, Proc. Natl. Acad. Sci. U.S.A. 94 (1997) 10249–10254.

[13] E. Schwarz, S. Benzer, The recently reported NIβ domain is already known as the Calx-β motif, Trends Biochem. Sci. 24 (1999) 260, https://doi.org/10.1016/S0968-0004(99)01422-X.

[14] J. Rizo, T.C. Südhof, C2-domains, structure and function of a universal Ca2+-binding domain, J. Biol. Chem. 273 (1998) 15879–15882, https://doi.org/10.1074/jbc.273.26.15879.

[15] A.L. Swain, R.H. Kretsinger, E.L. Amma, Restrained least squares refinement of native (calcium) and cadmium-substituted carp parvalbumin using X-ray crystallographic data at 1.6-Å resolution, J. Biol. Chem. 264 (1989) 16620–16628, https://doi.org/10.1016/S0021-9258(19)84751-8.

[16] D.A. Nicoll, The crystal structure of the primary Ca2+ sensor of the Na+/Ca2+ exchanger reveals a novel Ca2+ binding motif, J. Biol. Chem. 281 (2006) 21577–21581, https://doi.org/10.1074/jbc.C600117200.

[17] A.R. Pickford, I.D. Campbell, NMR studies of modular protein structures and their interactions, Chem. Rev. 104 (2004) 3557–3566, https://doi.org/10.1021/cr0304018.

[18] J.D. Walsh, K. Meier, R. Ishima, A.M. Gronenborn, NMR studies on domain diffusion and alignment in modular GB1 repeats, Biophys. J. 99 (2010) 2636–2646, https://doi.org/10.1016/j.bpj.2010.08.036.

[19] Y.E. Ryabov, D. Fushman, A model of interdomain mobility in a multidomain protein, J. Am. Chem. Soc. 129 (2007) 3315–3327, https://doi.org/10.1021/ja067667r.

[20] D. Chin, A.R. Means, Calmodulin: a prototypical calcium sensor, Trends Cell Biol. 10 (2000) 322–328, https://doi.org/10.1016/S0962-8924(00)01800-6.

[21] G. Barbato, M. Ikura, L.E. Kay, R.W. Pastor, A. Bax, Backbone dynamics of calmodulin studied by nitrogen-15 relaxation using inverse detected two-dimensional NMR spectroscopy: the central helix is flexible, Biochemistry 31 (1992) 5269–5278, https://doi.org/10.1021/bi00138a005.

[22] M. Ikura, G.M. Clore, A.M. Gronenborn, G. Zhu, C.B. Klee, A. Bax, Solution structure of a calmodulin-target peptide complex by multidimensional NMR, Science 256 (1992) 632–638, https://doi.org/10.1126/science.1585175.

[23] N. Tjandra, H. Kuboniwa, H. Ren, A. Bax, Rotational dynamics of calcium-free calmodulin studied by 15N-NMR relaxation measurements, Eur. J. Biochem. 230 (1995) 1014–1024, https://doi.org/10.1111/j.1432-1033.1995.tb20650.x.

[24] J.L. Baber, A. Szabo, N. Tjandra, Analysis of Slow interdomain motion of macromolecules using NMR relaxation data, J. Am. Chem. Soc. 123 (2001) 3953–3959, https://doi.org/10.1021/ja0041876.

[25] M. Zhang, T. Tanaka, M. Ikura, Calcium-induced conformational transition revealed by the solution structure of apo calmodulin, Nat. Struct. Mol. Biol. 2 (1995) 758–767, https://doi.org/10.1038/nsb0995-758.

[26] Y.S. Babu, C.E. Bugg, W.J. Cook, Structure of calmodulin refined at 2.2Å resolution, J. Mol. Biol. 204 (1988) 191–204, https://doi.org/10.1016/0022-2836(88)90608-0.

[27] H. Kuboniwa, N. Tjandra, S. Grzesiek, H. Ren, C.B. Klee, A. Bax, Solution structure of calcium-free calmodulin, Nat. Struct. Mol. Biol. 2 (1995) 768–776, https://doi.org/10.1038/nsb0995-768.

[28] B.E. Finn, J. Evenäs, T. Drakenberg, J.P. Waltho, E. Thulin, S. Forsén, Calcium-induced structural changes and domain autonomy in calmodulin, Nat. Struct. Mol. Biol. 2 (1995) 777–783, https://doi.org/10.1038/nsb0995-777.

[29] K.T. O'Neil, W.F. DeGrado, How calmodulin binds its targets: sequence independent recognition of amphiphilic α-helices, Trends Biochem. Sci. 15 (1990) 59–64, https://doi.org/10.1016/0968-0004(90)90177-D.

[30] W.E. Meador, A.R. Means, F.A. Quiocho, Target enzyme recognition by calmodulin: 2.4Å structure of a calmodulin-peptide complex, Science 257 (1992) 1251–1255, https://doi.org/10.1126/science.1519061.

[31] W.E. Meador, A.R. Means, F.A. Quiocho, Modulation of calmodulin plasticity in molecular recognition on the basis of X-ray structures, Science 262 (1993) 1718–1721, https://doi.org/10.1126/science.8259515.

[32] I. Bertini, C. Del Bianco, I. Gelis, N. Katsaros, C. Luchinat, G. Parigi, M. Peana, A. Provenzani, M.A. Zoroddu, Experimentally exploring the conformational space sampled by domain reorientation in calmodulin, Proc. Natl. Acad. Sci. U.S.A. 101 (2004) 6841–6846, https://doi.org/10.1073/pnas.0308641101.

[33] D.B. Heidorn, J. Trewhella, Comparison of the crystal and solution structures of calmodulin and troponin C, Biochemistry 27 (1988) 909–915, https://doi.org/10.1021/bi00403a011.

[34] G. Lipari, A. Szabo, Model-free approach to the interpretation of nuclear magnetic resonance relaxation in macromolecules. 1. Theory and range of validity, J. Am. Chem. Soc. 104 (1982) 4546–4559.

[35] L.E. Kay, D.A. Torchia, A. Bax, Backbone dynamics of proteins as studied by nitrogen-15 inverse detected heteronuclear NMR spectroscopy: application to staphylococcal nuclease, Biochemistry 28 (1989) 8972–8979.

[36] G.M. Clore, A. Szabo, A. Bax, L.E. Kay, P.C. Driscoll, A.M. Gronenborn, Deviations from the simple two-parameter model-free approach to the interpretation of nitrogen-15 nuclear magnetic relaxation of proteins, J. Am. Chem. Soc. 112 (1990) 4989–4991, https://doi.org/10.1021/ja00168a070.

[37] I. Bertini, C. Luchinat, G. Parigi, R. Pierattelli, NMR spectroscopy of paramagnetic metalloproteins, ChemBioChem. 6 (2005) 1536–1549, https://doi.org/10.1002/cbic.200500124.

[38] G. Pintacuda, M. John, X.-.C. Su, G. Otting, NMR structure determination of protein−ligand complexes by lanthanide labeling, Acc. Chem. Res. 40 (2011) 206–212, https://doi.org/10.1021/ar050087z.

[39] J.B. Stiller, R. Otten, D. Häussinger, P.S. Rieder, D.L. Theobald, D. Kern, Structure determination of high-energy states in a dynamic protein ensemble, Nature 603 (2022) 528–535, https://doi.org/10.1038/s41586-022-04468-9.

[40] T. Müntener, D. Joss, D. Häussinger, S. Hiller, Pseudocontact Shifts in Biomolecular NMR Spectroscopy, Chem. Rev. 122 (2022) 9422–9467, https://doi.org/10.1021/acs.chemrev.1c00796.

[41] E. Ravera, L. Salmon, M. Fragai, G. Parigi, H. Al-Hashimi, C. Luchinat, Insights into domain–domain motions in proteins and RNA from solution NMR, Acc. Chem. Res. 47 (2014) 3118–3126, https://doi.org/10.1021/ar5002318.

[42] X.-.C. Su, G. Otting, Paramagnetic labelling of proteins and oligonucleotides for NMR, J. Biomol. NMR 46 (2009) 101–112, https://doi.org/10.1007/s10858-009-9331-1.

[43] I. Bertini, I. Gelis, N. Katsaros, C. Luchinat, A. Provenzani, Tuning the affinity for lanthanides of calcium binding proteins, Biochemistry 42 (2003) 8011–8021, https://doi.org/10.1021/bi034494z.

[44] I. Bertini, Y.K. Gupta, C. Luchinat, G. Parigi, M. Peana, L. Sgheri, J. Yuan, Paramagnetism-based NMR restraints provide maximum allowed probabilities for the different conformations of partially independent protein domains, J. Am. Chem. Soc. 129 (2007) 12786–12794, https://doi.org/10.1021/ja0726613.

[45] D.Medeiros Selegato, C. Bracco, C. Giannelli, G. Parigi, C. Luchinat, L. Sgheri, E. Ravera, Comparison of different reweighting approaches for the calculation of conformational variability of macromolecules from molecular simulations, ChemPhysChem 22 (2021) 127–138, https://doi.org/10.1002/cphc.202000714.

[46] I. Bertini, A. Giachetti, C. Luchinat, G. Parigi, M.V. Petoukhov, R. Pierattelli, E. Ravera, D.I. Svergun, Conformational space of flexible biological macromolecules from average data, J. Am. Chem. Soc. 132 (2010) 13553–13558, https://doi.org/10.1021/ja1063923.

[47] L. Gigli, W. Andrałojć, A. Dalaloyan, G. Parigi, E. Ravera, D. Goldfarb, C. Luchinat, Assessing protein conformational landscapes: integration of DEER data in maximum occurrence analysis, Phys. Chem. Chem. Phys. 20 (2018) 27429–27438, https://doi.org/10.1039/C8CP06195E.

[48] W. Andrałojć, C. Luchinat, G. Parigi, E. Ravera, Exploring regions of conformational space occupied by two-domain proteins, J. Phys. Chem. B. 118 (2014) 10576–10587, https://doi.org/10.1021/jp504820w.

[49] L. Russo, M. Maestre-Martinez, S. Wolff, S. Becker, C. Griesinger, Interdomain dynamics explored by paramagnetic NMR, J. Am. Chem. Soc. 135 (2013) 17111–17120, https://doi.org/10.1021/ja408143f.

[50] N. Karschin, S. Becker, C. Griesinger, Interdomain Dynamics via paramagnetic NMR on the highly flexible complex calmodulin/Munc13-1, J. Am. Chem. Soc. (2022), https://doi.org/10.1021/jacs.2c06611 jacs.2c06611.

[51] L. Shapiro, W.I. Weis, Structure and Biochemistry of Cadherins and Catenins, Cold Spring Harb. Perspect. Biol. 1 (2009), https://doi.org/10.1101/cshperspect.a003053.

[52] B. Honig, L. Shapiro, Adhesion protein structure, molecular affinities, and principles of cell-cell recognition, Cell 181 (2020) 520–535, https://doi.org/10.1016/j.cell.2020.04.010.

[53] S.D. Patel, C. Ciatto, C.P. Chen, F. Bahna, M. Rajebhosale, N. Arkus, I. Schieren, T. M. Jessell, B. Honig, S.R. Price, L. Shapiro, Type II cadherin Ectodomain structures: implications for classical cadherin specificity, Cell 124 (2006) 1255–1268, https://doi.org/10.1016/j.cell.2005.12.046.

[54] B. Nagar, M. Overduin, M. Ikura, J.M. Rini, Structural basis of calcium-induced E-cadherin rigidification and dimerization, Nature 380 (1996) 360–364, https://doi.org/10.1038/380360a0.

[55] T.J. Boggon, J. Murray, S. Chappuis-Flament, E. Wong, B.M. Gumbiner, L. Shapiro, C-Cadherin Ectodomain structure and implications for cell adhesion mechanisms, Science 296 (2002) 1308–1313, https://doi.org/10.1126/science.1071559.

[56] S. Pokutta, K. Herrenknecht, R. Kemler, J. Engel, Conformational changes of the recombinant extracellular domain of E-cadherin upon calcium binding, Eur. J. Biochem. 223 (1994) 1019–1026, https://doi.org/10.1111/j.1432-1033.1994.tb19080.x.

[57] D. Häussinger, T. Ahrens, T. Aberle, J. Engel, J. Stetefeld, S. Grzesiek, Proteolytic E-cadherin activation followed by solution NMR and X-ray crystallography, EMBO J. 23 (2004) 1699–1708, https://doi.org/10.1038/sj.emboj.7600192.

[58] D. Häussinger, T. Ahrens, H.-.J. Sass, O. Pertz, J. Engel, S. Grzesiek, Calcium-dependent homoassociation of E-cadherin by NMr spectroscopy: changes in mobility, conformation and mapping of contact regions, J. Mol. Biol. 324 (2002) 823–839, https://doi.org/10.1016/S0022-2836(02)01137-3.

[59] M.R. Hansen, L. Mueller, A. Pardi, Tunable alignment of macromolecules by filamentous phage yields dipolar coupling interactions, Nat. Struct. Mol. Biol. 5 (1998) 1065–1074, https://doi.org/10.1038/4176.

[60] Y. Wu, X. Jin, O. Harrison, L. Shapiro, B.H. Honig, A. Ben-Shaul, Cooperativity between trans and cis interactions in cadherin-mediated junction formation, Proc. Natl. Acad. Sci. U.S.A. 107 (2010) 17592–17597, https://doi.org/10.1073/pnas.1011247107.

[61] O.J. Harrison, X. Jin, S. Hong, F. Bahna, G. Ahlsen, J. Brasch, Y. Wu, J. Vendome, K. Felsovalyi, C.M. Hampton, R.B. Troyanovsky, A. Ben-Shaul, J. Frank, S. M. Troyanovsky, L. Shapiro, B. Honig, The extracellular architecture of adherens junctions revealed by crystal structures of type I cadherins, Structure 19 (2011) 244–256, https://doi.org/10.1016/j.str.2010.11.016.

[62] V.Z. Miloushev, F. Bahna, C. Ciatto, G. Ahlsen, B. Honig, L. Shapiro, A. G. Palmer III, Dynamic properties of a type II cadherin adhesive domain: implications for the mechanism of strand-swapping of classical cadherins, Structure 16 (2008) 1195–1205, https://doi.org/10.1016/j.str.2008.05.009.

[63] H. Koss, B. Honig, L. Shapiro, A.G. Palmer, Dimerization of Cadherin-11 involves multi-site coupled unfolding and strand swapping, Structure 29 (2021) 1105–1115.e6, https://doi.org/10.1016/j.str.2021.06.006.

[64] O.J. Harrison, F. Bahna, P.S. Katsamba, X. Jin, J. Brasch, J. Vendome, G. Ahlsen, K. J. Carroll, S.R. Price, B. Honig, L. Shapiro, Two-step adhesive binding by classical cadherins, Nat. Struct Mol. Biol. 17 (2010) 348–357, https://doi.org/10.1038/nsmb.1784.
[65] Y. Li, N.L. Altorelli, F. Bahna, B. Honig, L. Shapiro, A.G. Palmer, Mechanism of E-cadherin dimerization probed by NMR relaxation dispersion, Proc. Natl. Acad. Sci. U.S.A. 110 (2013) 16462–16467, https://doi.org/10.1073/pnas.1314303110.
[66] D. Khananshvili, Sodium-calcium exchangers (NCX): molecular hallmarks underlying the tissue-specific and systemic functions, Pflugers Arch - Eur. J. Physiol. 466 (2014) 43–60, https://doi.org/10.1007/s00424-013-1405-y.
[67] L. Annunziato, G. Pignataro, G.F.D. Renzo, Pharmacology of brain Na+/Ca2+ exchanger: from molecular biology to therapeutic perspectives, Pharmacol. Rev. 56 (2004) 633–654, https://doi.org/10.1124/pr.56.4.5.
[68] K.D. Philipson, D.A. Nicoll, Sodium-calcium exchange: a molecular perspective, Annu. Rev. Physiol. 62 (2000) 111–133, https://doi.org/10.1146/annurev.physiol.62.1.111.
[69] J. Lytton, Na+/Ca2+ exchangers: three mammalian gene families control Ca2+ transport, Biochem. J. 406 (2007) 365–382, https://doi.org/10.1042/BJ20070619.
[70] A. Pannaccione, I. Piccialli, A. Secondo, R. Ciccone, P. Molinaro, F. Boscia, L. Annunziato, The Na+/Ca2+exchanger in Alzheimer's disease, Cell Calcium 87 (2020), 102190, https://doi.org/10.1016/j.ceca.2020.102190.
[71] J. Liao, H. Li, W. Zeng, D.B. Sauer, R. Belmares, Y. Jiang, Structural insight into the ion-exchange mechanism of the sodium/calcium exchanger, Science 335 (2012) 686–690, https://doi.org/10.1126/science.1215759.
[72] J. Liao, F. Marinelli, C. Lee, Y. Huang, J.D. Faraldo-Gómez, Y. Jiang, Mechanism of extracellular ion exchange and binding-site occlusion in a sodium/calcium exchanger, Nat. Struct. Mol. Biol. 23 (2016) 590–599, https://doi.org/10.1038/nsmb.3230.
[73] D. Khananshvili, Basic and editing mechanisms underlying ion transport and regulation in NCX variants, Cell Calcium 85 (2020), 102131, https://doi.org/10.1016/j.ceca.2019.102131.
[74] V. Breukels, W.G. Touw, G.W. Vuister, Structural and dynamic aspects of Ca2+ and Mg2+ binding of the regulatory domains of the Na+/Ca2+ exchanger, Biochem. Soc. Trans. 40 (2012) 409–414, https://doi.org/10.1042/BST20110742.
[75] M. Hilge, J. Aelen, G.W. Vuister, Ca2+ regulation in the Na+/Ca2+ exchanger involves two markedly different Ca2+ sensors, Mol. Cell. 22 (2006) 15–25, https://doi.org/10.1016/j.molcel.2006.03.008.
[76] G.M. Besserer, M. Ottolia, D.A. Nicoll, V. Chaptal, D. Cascio, K.D. Philipson, J. Abramson, The second Ca2+-binding domain of the Na+–Ca2+ exchanger is essential for regulation: crystal structures and mutational analysis, Proc. Natl. Acad. Sci. USA. 104 (2007) 18467–18472.
[77] M. Hilge, J. Aelen, A. Foarce, A. Perrakis, G.W. Vuister, Ca2+ regulation in the Na+/Ca2+ exchanger features a dual electrostatic switch mechanism, in: Proceedings of the National Academy of Sciences 106, 2009, pp. 14333–14338, https://doi.org/10.1073/pnas.0902171106.
[78] M. Giladi, Y. Sasson, X. Fang, R. Hiller, T. Buki, Y.-X. Wang, J.A. Hirsch, D. Khananshvili, A common Ca2+-driven interdomain module governs eukaryotic NCX regulation, PLoS ONE 7 (2012) e39985, https://doi.org/10.1371/journal.pone.0039985.
[79] M. Wu, S. Tong, J. Gonzalez, V. Jayaraman, J.L. Spudich, L. Zheng, Structural basis of the Ca2+ inhibitory mechanism of drosophila Na+/Ca2+ exchanger CALX and its modification by alternative splicing, Structure 19 (2011) 1509–1517, https://doi.org/10.1016/j.str.2011.07.008.
[80] M. Wu, M. Wang, J. Nix, L.V. Hryshko, L. Zheng, Crystal structure of CBD2 from the drosophila Na+/Ca2+ exchanger: diversity of Ca2+ Regulation and its alternative splicing modification, J. Mol. Biol. 387 (2009) 104–112, https://doi.org/10.1016/j.jmb.2009.01.045.
[81] M. Wu, H.D. Le, M. Wang, V. Yurkov, A. Omelchenko, M. Hnatowich, J. Nix, L. V. Hryshko, L. Zheng, Crystal structures of progressive Ca2+ binding states of the Ca2+ sensor Ca2+ binding domain 1 (CBD1) from the CALX Na+/Ca2+ exchanger reveal incremental conformational transitions, J. Biol. Chem. 285 (2010) 2554–2561, https://doi.org/10.1074/jbc.M109.059162.
[82] M. Mirdita, K. Schütze, Y. Moriwaki, L. Heo, S. Ovchinnikov, M. Steinegger, ColabFold: making protein folding accessible to all, Nat. Methods 19 (2022) 679–682, https://doi.org/10.1038/s41592-022-01488-1.
[83] E. Johnson, L. Bruschweiler-Li, S.A. Showalter, G.W. Vuister, F. Zhang, R. Brüschweiler, Structure and dynamics of Ca2+-binding domain 1 of the Na+/Ca2+ exchanger in the presence and in the absence of Ca2+, J. Mol. Biol. 377 (2008) 945–955, https://doi.org/10.1016/j.jmb.2008.01.046.
[84] V. Breukels, G.W. Vuister, Binding of calcium is sensed structurally and dynamically throughout the second calcium-binding domain of the sodium/calcium exchanger, Proteins 78 (2010) 1813–1824, https://doi.org/10.1002/prot.22695.
[85] R.K. Salinas, L. Bruschweiler-Li, E. Johnson, R. Bruschweiler, CA2+-binding alters the inter-domain flexibility between the two cytoplasmic calcium-binding domains in the NA+/CA2+ exchanger, J. Biol. Chem. 286 (2011) 32123–32131, https://doi.org/10.1074/jbc.M111.249268.
[86] L.A. Abiko, P.M. Vitale, D.C. Favaro, P. Hauk, D.-.W. Li, J. Yuan, L. Bruschweiler-Li, R.K. Salinas, R. Brüschweiler, Model for the allosteric regulation of the Na(+)/Ca(2+) exchanger NCX, Proteins 84 (2016) 580–590, https://doi.org/10.1002/prot.25003.
[87] M.V.C. Cardoso, J.D. Rivera, P.A.M. Vitale, M.F.S. Degenhardt, L.A. Abiko, C.L. P. Oliveira, R.K. Salinas, CALX-CBD1 Ca2+-binding cooperativity studied by NMR spectroscopy and ITC with Bayesian statistics, Biophys. J. 119 (2020) 337–348, https://doi.org/10.1016/j.bpj.2020.05.031.
[88] M.F. de Souza Degenhardt, P.A.M. Vitale, L.A. Abiko, M. Zacharias, M. Sattler, C.L. P. Oliveira, R.K. Salinas, Molecular insights on CALX-CBD12 interdomain dynamics from MD simulations, RDCs, and SAXS, Biophys. J. (2021), https://doi.org/10.1016/j.bpj.2021.07.022. S0006349521006081.
[89] P. Bernadó, E. Mylonas, M.V. Petoukhov, M. Blackledge, D.I. Svergun, Structural characterization of flexible proteins using small-angle X-ray scattering, J. Am. Chem. Soc. 129 (2007) 5656–5664, https://doi.org/10.1021/ja069124n.
[90] D.W. Hilgemann, Regulation and deregulation of cardiac Na+-Ca2+ exchange in giant excised sarcolemmal membrane patches, Nature 344 (1990) 242–245, https://doi.org/10.1038/344242a0.
[91] C. Dyck, K. Maxwell, J. Buchko, M. Trac, A. Omelchenko, M. Hnatowich, L. V. Hryshko, Structure-function analysis of CALX1.1, a Na+-Ca2+ exchanger from Drosophila, J. Biol. Chem. 273 (1998) 12981–12987, https://doi.org/10.1074/jbc.273.21.12981.
[92] L.V. Hryshko, Anomalous regulation of the Drosophila Na(+)-Ca2+ exchanger by Ca2+, J. Gen. Physiol. 108 (1996) 67–74, https://doi.org/10.1085/jgp.108.1.67.
[93] M. Ottolia, D.A. Nicoll, K.D. Philipson, Roles of two Ca2+-binding domains in regulation of the cardiac Na+-Ca2+ exchanger, J. Biol. Chem. 284 (2009) 32735–32741, https://doi.org/10.1074/jbc.M109.055434.
[94] J. Yuan, C. Yuan, M. Xie, L. Yu, L. Bruschweiler-Li, R. Brüschweiler, The intracellular loop of the Na+/Ca2+ exchanger contains an "Awareness Ribbon"-Shaped two-helix bundle domain, Biochemistry 57 (2018) 5096–5104, https://doi.org/10.1021/acs.biochem.8b00300.
[95] C. Eichmüller, N.R. Skrynnikov, Observation of μs time-scale protein dynamics in the presence of Ln3+ ions: application to the N-terminal domain of cardiac troponin C, J. Biomol. NMR 37 (2007) 79–95, https://doi.org/10.1007/s10858-006-9105-y.
[96] E. Ravera, L. Sgheri, G. Parigi, C. Luchinat, A critical assessment of methods to recover information from averaged data, Phys. Chem. Chem. Phys. 18 (2016) 5686–5701, https://doi.org/10.1039/C5CP04077A.